InPrime: Indonesian Journal of Pure and Applied Mathematics
Vol. 5, No. 1 (2023), pp. 22 – 37, doi: 10.15408/inprime.v5i1.27205
p-ISSN 2686-5335, e-ISSN: 2716-2478

Stability Analysis and Optimal Control of Mathematical Model of Thypoid Fever Spread

Muh. Nursyam Siduppa, Syamsuddin Toaha, and Kasbawati*
Department of Mathematics, Hasanuddin University, Makassar, Indonesia
Email: muh.nursyamsiduppa09@gmail.com, syamsuddint@unhas.ac.id, *kasbawati@unhas.ac.id

Abstract

Typhoid fever is an endemic disease caused by infection with Salmonella Typhi. The transmission of typhoid fever is through food and drink contaminated with Salmonella Typhi bacteria, which is excreted through the feces or urine of an infected person. The problem of typhoid fever is increasingly complex because of the increase in carrier cases, making it difficult for treatment and prevention efforts. This study develops a mathematical model for the control of typhoid fever, which consists of two equilibrium points, namely endemic and non-endemic equilibrium points. The endemic and non-endemic equilibrium point is asymptotically stable if it satisfies the condition given by the Routh-Hurwitz criterion. Optimal control theory is applied to the mathematical model by providing control through health campaigns, screening, and treatment to minimize the number of asymptomatic individuals, symptomatic individuals, and chronic carriers. The Pontryagin Minimum principle is used to determine the optimal control form. Numerical simulations are performed using the Forward-Backward Sweep Runge-Kutta method of order 4. The simulation results indicate a decrease in each infected subpopulation after applying optimal control for ten months. It is found that control in health campaigns has a more significant impact than control in screening and treatment in decreasing the number of asymptomatic and symptomatic individuals. The control of treatment effectively reduces infected individuals with symptoms of becoming chronic carriers. In conclusion, the most effective strategy in controlling the spread of typhoid fever is to simultaneously apply controls in the form of health campaigns, screening, and treatment.

Keywords: health campaign; screening; treatment; optimal control; Pontryagin minimum principle; forward-backward sweep.

Abstrak

Demam tifoid merupakan penyakit endemik yang disebabkan oleh infeksi bakteri Salmonella Typhi. Proses penularan demam tifoid melalui makanan dan minuman yang telah terkontaminasi bakteri Salmonella Typhi yang dikeluarkan melalui tinja maupun urin dari orang yang telah terinfeksi. Permasalahan tentang demam tifoid semakin kompleks karena meningkatnya kasus - kasus carrier, sehingga menyulitkan upaya pengobatan dan pencegahan. Model matematika yang dikembangkan memiliki dua titik kesetimbangan yaitu titik setimbang nonendemik dan titik setimbang endemik. Titik setimbang nonendemik dan endemik akan stabil asimtotik jika memenuhi kondisi yang diberikan oleh aturan Routh-Hurwitz. Teori kontrol optimal diterapkan pada model matematika dengan pemberian kontrol berupa kampanye kesehatan, screening dan pengobatan untuk meminimumkan jumlah individu asymptomatic, individu symptomatic dan carrier chronic. Penentuan bentuk kontrol optimal menggunakan prinsip Minimum Pontryagin. Simulasi numerik dilakukan dengan menggunakan metode Forward-Backward Sweep Runge-Kutta orde 4. Berdasarkan hasil simulasi, terjadi penurunan disetiap subpopulasi terinfeksi setelah penerapan kontrol optimal selama 10 bulan. Kontrol berupa kampanye kesehatan memiliki pengaruh yang besar dibandingkan kontrol berupa screening dan pengobatan dalam menekan meningkatnya individu asymptomatic dan individu symptomatic. Penerapan

* Corresponding author
Submitted July 19th, 2022, Revised February 3rd, 2023, Accepted for publication February 16th, 2023.

kontrol berupa pengobatan sangat efektif dalam menekan individu terinfeksi dengan gejala menjadi individu carrier chronic.
Kata Kunci: *kampanye kesehatan;* screening; *pengobatan; kontrol optimal; prinsip minimum Pontryagin;* forward-backward sweep.

2020MSC: 00A71, 92B05

1. INTRODUCTION

According to [1], typhoid fever often occurs in several countries worldwide and generally occurs in developing countries with low levels of hygiene. Typhoid fever is a public health problem, with cases reaching 11-20 million yearly, resulting in around 128.000-161.000 deaths annually [2]. Typhoid fever is an endemic disease in Indonesia, caused by infection with Salmonella Typhi bacteria. These bacteria can be transmitted through food and drink contaminated with Salmonella Typhi bacteria which are excreted through feces and urine from people infected with Salmonella Typhi bacteria [3], [4], [5]. Typhoid fever is a disease that must receive serious attention from various parties because it is endemic and threatens public health [6]. According to [7], the problem of typhoid fever is increasingly complex, with increasing carrier cases, relapses, and resistance to the drugs used, making it difficult for treatment and prevention efforts. After treatment, not all patients recover completely. Approximately 2% - 4% of typhoid fever patients become carrier chronic. These patients remain asymptomatic after acute treatment, but they can excrete Salmonella Typhi bacteria for up to 1 year in feces and urine [5], [8], [9], [10].

The study of typhoid fever and strategies for controlling the spread of typhoid fever can be done theoretically, one of which is through mathematical modeling. Mathematical modeling is widely used to describe various real problems in everyday life and various fields, including the health sector. For example, the mathematical model spreads infectious diseases. In connection with these problems, mathematical models can be used to determine the dynamics spread of disease. Thus, an effective strategy can be determined to control the disease. According to [11], the mathematical model has been widely used as an approach to identify the mechanism spread of disease properly. At the same time, optimal control is a standard method used to solve optimization problems of a continuous dynamic system. The definition of the objective function is based on the goals to be achieved [12].

Research on the spread of typhoid fever was previously carried out by several researchers, including [13], [14], [15], [16], [17], [18], [19]. In this study, a mathematical model of the spread of typhoid fever is developed [15] by reviewing the impact and influence of chronic carriers and their impact on the spread of typhoid fever. This current study develops a mathematical model by adding a chronic carrier individual (C).

2. METHODS

The mathematical model of the spread of typhoid fever in this article is the development of a mathematical model [15] by adding the Carrier Chronic compartment. Therefore, this study consists of six compartments, namely: susceptible individuals (S), asymptomatic infection individuals (I_c),

symptomatic infection individuals (I), chronic carrier individuals (C), Recovered Individuals (R) and population of Salmonella Typhi bacteria in the environment (B).

Susceptible individuals (S) will increase due to natural birth at the rate of Λ. Typhoid fever is transmitted from bacteria in the environment through food or water contaminated by the Salmonella typhi bacteria [13], [15], [16], so the case of new infections is $\frac{\boldsymbol{vB}}{\boldsymbol{K+B}}$, v is the rate of absorption of Salmonella Typhi bacteria in food or drink, K is the concentration of Salmonella Typhi bacteria in food and beverages. Individuals who consume food or drink contaminated with Salmonella Typhi bacteria have a probability of ρ to getting into asymptomatic infection individuals (I_c) or $(1-\rho)$ to getting into symptomatic infection individuals (I).

Asymptomatic infection individuals (I_c) will get into symptomatic infection individuals I after screening with the rate of θ, while ϕ is the natural recovered rate in asymptomatic infection individuals (I_c). It is assumed that the natural death rate in each sub-population is the same, which is μ. Death due to disease only occurs in symptomatic individuals (I) with the rate of δ. Recovered after treatment is divided into two: complete recovery and not full recovery. Individuals who recover completely after treatment enter Recovery individuals (R) at the rate of τ. Individuals who do not fully recover will enter the Chronic Carrier individuals(C) at the rate of β. At the same time, α is the natural recovery rate in Chronic Carrier individuals (C). Salmonella typhi bacteria population in the environment (B) will increase due to bacterial removal from asymptomatic infection individuals (I_c) through feces and urine with an abacterial removal rate of η_1, symptomatic infection individuals (I) with the rate of η_2 and Chronic Carrier individuals C with the rate of η_3.

Salmonella typhi bacteria population(B) in the environment will be decreased due to the natural death of bacteria at the rate of μ_b. Early prevention is needed in controlling the disease to reduce the rate of entry of susceptible individuals (S) into asymptomatic infection individuals (I_c) and symptomatic infection individuals (I) implementing health campaigns control (u_1), which shows the success of the health campaigns while $(1-u_1)$ shows unsuccessful in health campaigns. To obtain appropriate treatment, asymptomatic infection individuals (I_c) have to do screening (u_2), and to decrease the number of symptomatic infection individuals (I) and Chronic Carrier individuals (C), then complete treatment must be carried out (u_3). Based on the assumptions, the changes that occur for each population in the spread of typhoid fever can be seen in Figure 1. Based on this figure, the model for the spread of typhoid fever is as follows:

$$
\begin{aligned}
\frac{dS}{dt} &= \Lambda + \varepsilon R - (1-u_1)\frac{vB}{K+B}S - \mu S,\\
\frac{dI_c}{dt} &= (1-u_1)\frac{\rho vB}{K+B}S - (\phi + u_2 + \theta + \eta_1 + \mu)I_c,\\
\frac{dI}{dt} &= (1-u_1)\frac{(1-\rho)vB}{K+B}S + (1-u_2)\theta I_c - (\tau + u_3 + \beta + \eta_2 + \delta + \mu),\\
\frac{dC}{dt} &= \beta I - (\alpha + u_3 + \eta_3 + \mu)C,\\
\frac{dR}{dt} &= \phi I_c + (\tau + u_3)I + (\alpha + u_3 C) - (\varepsilon + \mu)R,
\end{aligned}
\tag{1}
$$

$$\frac{dB}{dt} = \eta_1 I_c + \eta_2 I + \eta_3 C - \mu_b B.$$

The variables and parameters in the model (1) are presented in Table 1 and Table 2.

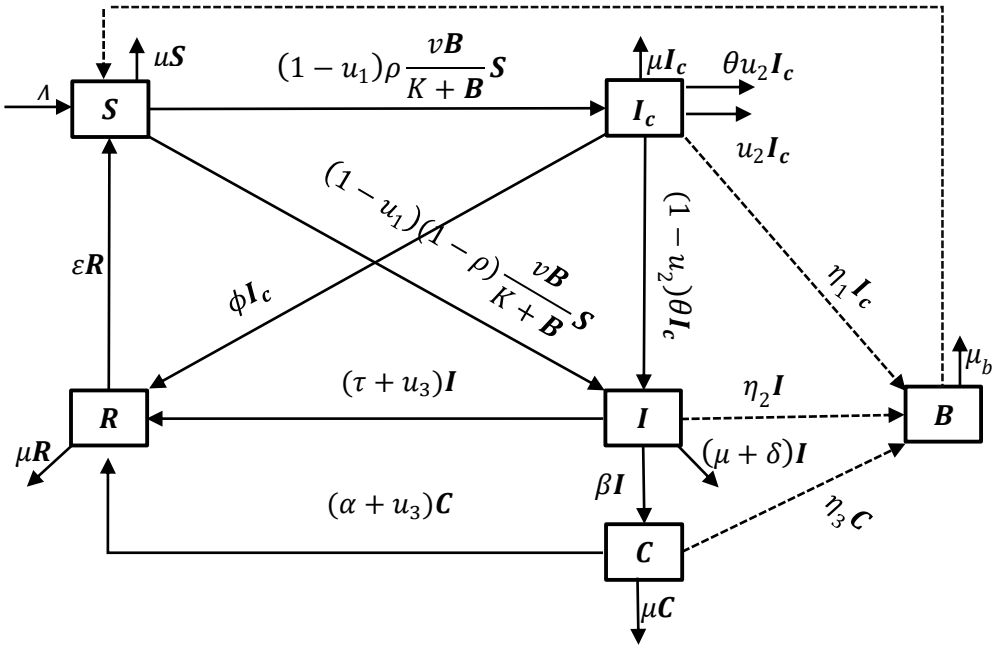

Figure 1. Compartment diagram of the spread of typhoid fever

Table 1. Variables in the model (1)

Variable	Description	Unit
$S(t)$	Number of susceptible individuals infected with typhoid fever	Person
$I_c(t)$	Number of individuals infected with typhoid fever without showing symptoms	Person
$I(t)$	Number of individuals infected with typhoid fever with symptoms	Person
$C(t)$	Number of individuals who made treatment but still had Salmonella Typi bacteria in their intestines	Person
$R(t)$	Number of individuals who recovered from typhoid fever	Person
$B(t)$	The population of Salmonella Typhi bacteria in the environment	Bacteria

Table 2. Parameters in the Model (1)

Parameter	Description	Value	Reference
Λ	Human birth rate	100	[15]
μ	Natural mortality rate	0.0247	[15]
ε	The rate of losing the natural immunity of humans	0.000904	[15]
ρ	Probability of individuals entering the class of asymptomatic infection	0.3	[15]
K	The concentration of Salmonella Typhi bacteria in food and beverages	50000	[15]
ν	The absorption rate of Salmonella Typhi bacteria in humans	0.9	[15]
θ	Screening rate	0.2	[15]

Table 2. Continued

Parameter	Description	Value	Reference
ϕ	The natural recovery rate of the asymptomatic infection population	0.0003	[15]
δ	The mortality rate due to typhoid fever	0.052	[15]
τ	Recovery rate	0.002	[15]
α	The natural recovery rate of Carrier Chronic individuals	0.0834	[20]
μ_b	The natural mortality rate of Salmonella Typhi Bacteria	0.001	[15]
η_1	The rate of removal of Salmonella Typhi Bacteria from the asymptomatic infection population	0.9	[15]
η_3	The rate of removal of Salmonella Thypi Bacteria from the Carrier Chronic population	0.01	[21]
β	The rate from symptomatic infection population to Carrier Chronic individuals	0.004	[16]
η_2	The rate of removal of Salmonella Thypi Bacteria from the symptomatic infection population	0.8	[15]
u_1	The successful proportion of the health campaign of the population (S), $0 \leq u_1 \leq 1$.	-	
u_2	Screening proportion, $0 \leq u_2 \leq 1$	-	
u_3	The proportion of successful treatment, $0 \leq u_3 \leq 1$.	-	

3. RESULTS AND DISCUSSION

3.1 The Equilibrium Point of the Model

The non-endemic equilibrium point is a condition where the disease does not spread in a population. The condition occurs when $I_c = I = C = B = 0$. By substituting and solving for each variable in (1), the disease-free equilibrium point is obtained as follows:

$$E^0 = \left(S^0,\ {I_c}^0,\ I^0,\ C^0,\ B^0,\ R^0\right) = \left(\frac{\Lambda}{\mu}, 0,0,0,0,0\right).$$

The endemic equilibrium point is the condition when the disease spreads in a population. The condition occurs when ${I_c}^* > 0,\ I^* > 0,\ C^* > 0, R^* > 0,$ and $B^* > 0$. Then, by using the equation of (1) obtained:

$$E^* = (S^*,\ {I_c}^*,\ I^*,\ C^*,\ B^*,\ R^*),$$

where

$$S^* = \frac{L_3 L_4 L_7 \Lambda}{L_4 L_3 L_6 L_7 (L_1 L_2 + \mu) - L_1 L_2 L_4 \rho \varepsilon L_6 \phi - L_1 L_2 \varepsilon \left(L_6 L_{10} + \beta L_{11}\right)(L_9 \rho + L_8 L_3)},$$

$$I_c^* = \frac{L_4 \rho L_1 L_2 L_6 L_7 \Lambda}{L_4 L_3 L_6 L_7 (L_1 L_2 + \mu) - L_1 L_2 L_4 \rho \varepsilon L_6 \phi - L_1 L_2 \varepsilon (L_6 L_{10} + \beta L_{11})(L_9 \rho + L_8 L_3)},$$

$$I^* = \frac{L_1 L_2 L_6 L_7 \Lambda (L_9 \rho + L_8 L_3)}{L_4 L_3 L_6 L_7 (L_1 L_2 + \mu) - L_1 L_2 L_4 \rho \varepsilon L_6 \phi - L_1 L_2 \varepsilon (L_6 L_{10} + \beta L_{11})(L_9 \rho + L_8 L_3)},$$

$$C^* = \frac{\beta L_1 L_2 L_7 \Lambda (L_9\rho + L_8 L_3)}{L_4 L_3 L_6 L_7 (L_1 L_2 + \mu) - L_1 L_2 L_4 \rho \varepsilon L_6 \phi - L_1 L_2 \varepsilon (L_6 L_{10} + \beta L_{11})(L_9\rho + L_8 L_3)},$$

$$R^* = \frac{L_3 L_4 L_7 \Lambda (L_1 L_2 + \mu)}{\varepsilon L_4 L_3 L_6 L_7 (L_1 L_2 + \mu) - \varepsilon L_1 L_2 L_4 \rho \varepsilon L_6 \phi - \varepsilon L_1 L_2 \varepsilon \left(L_6 L_{10} + \beta L_{11}\right)(L_9\rho + L_8 L_3)} - \frac{\Lambda}{\varepsilon},$$

$$B^* = \frac{\eta_1 I^*_c + \eta_2 I^* + \eta_3 C^*}{\mu_b},$$

with $L_1 = (1-u_1)$, $L_2 = \frac{\nu B}{k+B}$, $L_3 = \left(\phi + u_2 + \theta + \eta_1 + \mu\right)$, $L_4 = \left(\tau + \eta_2 + \delta + \mu\right)$, $L_5 = (1-u_3)$, $L_6 = \left(\alpha + \eta_3 + \mu\right)$, $L_7 = (\varepsilon + \mu)$, $L_8 = (1-\rho)$, $L_9 = (1-u_2)\theta$, $L_{10} = \tau + u_3$, $L_{11} = \alpha + u_3$.

3.2 Stability Analysis of the Model

By linearizing the system (1), the Jacobian matrix is

$$J = \begin{pmatrix} -(1-u_1)\frac{\nu B}{K+B} - \mu & 0 & 0 & 0 & \varepsilon & -(1-u_1)\frac{K\nu}{(K+B)^2}S \\ (1-u_1)\frac{\rho\nu B}{K+B} & -\left(\phi + u_2 + \theta + \eta_1 + \mu\right) & 0 & 0 & 0 & (1-u_1)\frac{\rho K\nu}{(K+B)^2}S \\ (1-u_1)\frac{(1-\rho)\nu B}{K+B} & (1-u_2)\theta & -\left(\tau + u_3 + \eta_2 + \beta + \delta + \mu\right) & 0 & 0 & (1-u_1)\frac{(1-\rho)K\nu}{(K+B)^2}S \\ 0 & 0 & \beta & -\left(\alpha + u_3 + \eta_3 + \mu\right) & 0 & 0 \\ 0 & \phi & \tau + u_3 & \alpha + u_3 & -(\varepsilon + \mu) & 0 \\ 0 & \eta_1 & \eta_2 & \eta_3 & 0 & -\mu_b B \end{pmatrix}.$$

Then, the stability of the disease-free equilibrium point will be analyzed (E^0) by evaluating the Jacobian matrix at the non-endemic equilibrium point and solving the characteristic equation of $det\left(\lambda I - J(E^0)\right) = 0$ so that the eigenvalue is obtained λ , which is a solution of the characteristic equation (2).

$$(\lambda + \mu)(\lambda + L_7)(\lambda^4 + A_1\lambda^3 + A_2\lambda^2 + A_3\,\lambda + \mathrm{A}_4\,) = 0. \tag{2}$$

From the characteristic equation (2) it is obtained $\lambda_1 = -\mu$ and $\lambda_2 = -L_7$, the other four eigenvalues are obtained by solving the characteristic equation,

$$\lambda^4 + A_1\lambda^3 + A_2\lambda^2 + A_3\,\lambda + A_4 = 0, \tag{3}$$

with $A_1 = (L_3 + L_4 + L_6 + \mu_b)$, $A_2 = \left((L_3 + L_4 + \mu_b)L_6 + (L_4 + \mu_b)L_3 + L_4\mu_b\right) - \frac{L_1\nu\Lambda}{K\mu}(\mathrm{L}_8\eta_2 + \eta_1\rho)$,

$A_3 = \left(\left((L_4 + \mu_b)L_3 + L_4\mu_b\right)L_6 + L_3L_4\mu_b\right) - \frac{\Lambda L_1\nu}{K\mu}\left((\mathrm{L}_8\eta_2 + \eta_2\rho)L_6 + \tau\eta_3L_5L_8 + \eta_1\rho L_4 + \eta_2\rho + \eta_2L_3L_8\right)$, $A_4 = (\mathrm{L}_3L_4L_6\mu_b - \left(\left(\eta_2L_3L_8 + \rho(\eta_1L_4 + \eta_2\rho)\right)L_6 + \tau\eta_3L_5(L_3L_8 + \rho)\right)\frac{\Lambda\nu L_1}{K\mu}$.

The characteristic equation (3) solution is difficult to obtain explicitly because it involves many parameters. By using the Routh-Hurwitz criterion, non-endemic equilibrium point E^0 will be asymptotically stable if the polynomial (3) has roots with a negative real part if it satisfies the condition:

$$A_1, A_2, A_3, A_4 > 0 \text{ and } A_1A_2A_3A_4 > A_1^2A_4^2 + A_3^2A_4 .$$

We get linearization around the endemic equilibrium point by evaluating the Jacobian matrix at the endemic equilibrium point (E^*). Eigenvalue λ is obtained by solving the characteristic equation $det(\lambda I - J(E^*)) = 0$.

$$\lambda^6 + A_1\lambda^5 + A_2\lambda^4 + A_3\lambda^3 + A_4\lambda^2 + A_5\lambda + A_6 = 0, \tag{4}$$

with

$A_1 = (L_3 + L_4 + L_6 + L_7 + M_1 + \mu_b),$

$A_2 = \big((L_3 + \mu_b + L_4 + L_7 + M_1)L_6 + (L_3 + \mu_b + L_4 + M_1)L_7 + (L_3 + L_4 + \mu_b)M_1 + (L_4 + \mu_b)L_3 + L_4\mu_b - \eta_1x_2 - \eta_2x_3\big),$

$A_3 = \Big(\big((L_3 + \mu_b + L_4 + M_1)L_7 + (L_3 + \mu_b + L_4)M_1 + (L_4 + \mu_b)L_3 + L_4\mu_b - \eta_1x_2 - \eta_2x_3\big)L_6 + (((L_3 + \mu_b + L_4)M_1 + (L_4 + \mu_b)L_3 + L_4\mu_b - \eta_1x_2 - \eta_2x_3)L_7 + \big((L_4 + \mu_b)L_3 + L_4\mu_b - \eta_1x_2 - \eta_2x_3\big)M_1 + (L_4\mu_b - \eta_2x_3)L_3 - L_4x_2\eta_1 + (M_3x_1 - x_2L_9)\eta_2 + (-M_2\phi - M_3L_{10})\varepsilon + M_2\eta_1x_1 - \beta\eta_3x_3\Big),$

$A_4 = \Big(\Big(\big((L_3 + L_4 + \mu_b)M_1 + (L_4 + \mu_b)L_3 + L_4\mu_b - \eta_1x_2 - \eta_2x_3\big)L_7 + \big((L_4 + \mu_b)L_3 + L_4\mu_b - \eta_1x_2 - \eta_2x_3\big)M_1 + (L_4\mu_b - \eta_2x_3)L_3 - L_4x_2\eta_1 + (M_3x_1 - x_2L_9)\eta_2 + (-M_2\phi - M_3N_2)\varepsilon + M_2\eta_1x_1\Big)L_6 + \Big(\big((L_4 + \mu_b)L_3 + L_4\mu_b - \eta_1x_2 - \eta_2x_3\big)M_1 + (L_4\mu_b - \eta_2x_3)L_3 - L_4x_2\eta_1 + (M_3x_1 - x_2L_9\big)\eta_2 + M_2\eta_1x_1 - N_1\eta_3x_3\Big)L_7 + \big((L_4\mu_b - \eta_2x_3)L_3 - x_2L_9\eta_2 - L_4x_2\eta_1 - N_1\eta_3x_3\big)M_1 + (-M_3N_2\varepsilon + M_3\eta_2x_1 - N_1\eta_3x_3)L_3 + M_2(\eta_1x_1 - \varepsilon\phi)L_4 - \varepsilon\mu_b(M_2\phi + M_3N_2) + M_2\eta_2x_1L_9 + (-M_2L_9L_{10} - M_3\beta L_{11})\varepsilon + \eta_3\beta(M_3x_1 - x_2L_9)),$

$A_5 = \Big(\Big(\big((L_4 + \mu_b)L_3 + L_4\mu_b - \eta_1x_2 - \eta_2x_3\big)M_1 + (L_4\mu_b - \eta_2x_3)L_3 - L_4x_2\eta_1 + (M_3x_1 - x_2L_9)\eta_2 + M_2\eta_1x_1\Big)L_7 + \big((L_4\mu_b - \eta_2x_3)L_3 - x_2(L_4\eta_1 + \eta_2L_9)\big)M_1 + M_3(-L_{10}\varepsilon + \eta_2x_1)L_3 + M_2(\eta_1x_1 - \varepsilon\phi)L_4 - \varepsilon\,\mu_b(M_2\phi + M_3N_2) + L_9M_2(-L_{10}\varepsilon + x_1\eta_2)\Big)L_6 + \Big(\big((L_4\mu_b - \eta_2x_3)L_3 - x_2L\eta_2 - L_4x_2\eta_1 - \beta\eta_3x_3\big)M_1 + (M_3\eta_2x_1 - N_1\eta_3x_3)L_3 + L_4M_2x_1\eta_1 + M_2\eta_2L_9x_1 + \eta_3\beta(M_3x_1 - x_2L_9)\Big)L_7 - \beta\eta_3M_1(L_3x_3 + x_2L_9) - M_3\big(\mu_b\boldsymbol{\varepsilon L_{10}} - \beta(\eta_3x_1 - L_{11}\varepsilon)\big)L_3 - L_4M_2\mu_b\varepsilon\phi - \varepsilon(M_3L_9L_{10} + M_3\beta L_{11})\mu_b - \varepsilon\phi(-M_2x_3 + M_3x_2)\eta_2 + \big((-\beta L_9L_{11} - L_{10}x_3\eta_1)M_2 + M_3\eta_1x_2L_{10}\big)\varepsilon + M_2\eta_3x_1L_9),$

$A_6 = (\Big(\big((L_4\mu_b - \eta_2x_3)L_3 - x_2(L_4\eta_1 + \eta_2L_9)\big)M_1 + (M_3\eta_2L_3 + M_2(L_4\eta_1 + \eta_2L_9)x_1)L_7 - \varepsilon\big(L_3M_3L_{10}\mu_b + L_4M_2\mu_b\phi + M_2L_9L_{10}\mu_b + (-L_{10}\eta_1 + \phi\eta_2)(-M_2x_3 + M_3x_2)\big)\Big)L_6 - \big(-\eta_3\big((-L_3x_3 - x_2L_9)M_1 + x_1(M_3L_3 + M_2L_9)\big)L_7 + \big(L_3\mu_bL_{11}M_3 + \mu_bL_9L_{11}M_2 + (-L_{11} + \eta_3\phi)(-M_2x_3 + M_3x_2)\big)\varepsilon\big).$

By using the Routh-Hurwitz criterion, endemic equilibrium point E^* will be asymptotically stable if the polynomial (4) has roots with a negative real part if it satisfies the condition:

$A_1, A_2, A_3, A_4, A_5, A_6 > 0$ and $A_1A_2A_3A_4A_5A_6 + A_2A_3A_5^2A_6 + 2A_1A_4A_5^2A_6 + A_3^2A_6^2 + A_1^2A_3A_4A_6^2 + 2A_1^2A_2A_5A_6^2 > A_3^2A_4A_5A_6 + A_1^2A_4^2A_5A_6 + A_1A_2^2A_5^2A_6 + A_5^3A_6 + A_1A_2A_3^2A_6^2 + 3A_1A_3A_5A_6^2 + A_1^3A_6^3$.

3.3 Formulation and Optimal Control Solution

In this model, optimal control theory is applied to obtain the control function of health campaigns(u_1), *screening* (u_2), and treatment (u_3) so that it can reduce infected individuals without symptoms (I_c), infected individuals with symptoms(I), and chronic carrier individuals. Control function $u_i(t)$, $i = 1,2,3$ defined in area $0 \le u_i(t) \le 1$, for each $t \in [t_0, t_f]$. The value of $u_i(t) = 0$ shows that the given control is inefficient for being applied, and the value of $u_i(t) = 1$ shows that the given control is very efficient. t_0 is the initial time of providing control, and t_f is the end time of giving control. Then we get three control functions defined in the determined area, as follows:

$$U = \{(u_1(t), u_2(t), u_3(t)) | 0 \le u_1 \le 1, 0 \le u_2 \le 1, 0 \le u_3 \le 1, \quad t \in [t_0, t_f]\}.$$

The relationship between the costs to be incurred for each control variable $u_i(t)$ with the number of infected individual populations in the form of non-linear so that the cost function is formed in a quadratic model $\frac{1}{2}W_iu_i^2(t)$, $i = 1,2,3$ with W_i is the weight that is correlated with the costs incurred for each control variable than the value of $\frac{1}{2}$ stating the importance of the expenses concerned are identical. A_i, $i = 1,2,3$ is the weight of each infected subpopulation. Based on the description above, the following objective functions can be formed:

$$T = \min_{(u_1,u_2,\boldsymbol{u_3})} \int_0^{t_f} \left(A_1I_c + A_2I + A_3C + \frac{1}{2}\sum_{i=1}^{3} W_i{u_i}^2 \right) dt,$$

$$T = \min_{(u_1,u_2,\boldsymbol{u_3})} \int_0^{t_f} \left(A_1I_c + A_2I + A_3C + \frac{1}{2}(W_1{u_1}^2 + W_2{u_2}^2 + W_3{u_3}^2) \right) dt.$$

Determination of optimal control $\boldsymbol{u}^*$ is done using Pontryagin's minimum principle. The first thing to do is to form a Hamiltonian function [22]. The general form of the Hamiltonian function:

$$H(t, \boldsymbol{x}, u, \boldsymbol{\lambda}) = f(t, \boldsymbol{x}, u) + \boldsymbol{\lambda^T}(t)\boldsymbol{g}(t, \boldsymbol{x}, u). \tag{5}$$

Let the Lagrange multiplier in equation (5) as:

$$\boldsymbol{\lambda} = (\lambda_1 \ \lambda_2 \ \lambda_3 \ \lambda_4 \ \lambda_5 \lambda_6)^{\boldsymbol{T}}.$$

Then,

$$f(t, \boldsymbol{x}, u) = A_1I_c + A_2I + A_3C + \frac{1}{2}w_1{u_1}^2 + \frac{1}{2}w_2{u_2}^2 + \frac{1}{2}w_3{u_3}^2.$$

Based on equation (5), a Hamiltonian function can be formed such as equation (6):

$$H = A_1 I_c + A_2 I + A_3 C + \frac{1}{2} w_1 {u_1}^2 + \frac{1}{2} w_2 {u_2}^2 + \frac{1}{2} w_3 {u_3}^2 + \lambda_1 \left(\Lambda + \varepsilon R - \left(\left(1 - u_1(t)\right)\frac{\nu B}{K+B} + \mu\right) S\right) + \lambda_2 \left(\left(1 - u_1(t)\right)\frac{\rho \nu B}{K+B} S - (\phi + u_2(t) + \theta + \eta_1 + \mu) I_c\right) + \lambda_3 \left((1 - u_1)\frac{(1-\rho)\nu B}{K+B} S + (1 - u_2(t))\theta I_c - (\tau + u_3(t) + \beta + \eta_2 + \delta + \mu) I\right) + \lambda_4 (\beta I - (\alpha + u_3(t) + \eta_3 + \mu) C) + \lambda_5 (\phi I_c + (\tau + u_3(t)) I + (\alpha + u_3(t)) C - (\varepsilon + \mu) R) + \lambda_6 (\eta_1 I_c + \eta_2 I + \eta_3 C - \mu_b B). \quad (6)$$

The Hamiltonian equation (6) will determine the equation of state, costate and stationary conditions of (1). By drifting the Hamiltonian equation (6) to the Lagrange multiplier, we get the state equation:

$$\dot{\boldsymbol{x}} = \frac{\partial H}{\partial \boldsymbol{\lambda}} = \left(\frac{\partial H}{\partial \lambda_1} \;\; \frac{\partial H}{\partial \lambda_2} \;\; \frac{\partial H}{\partial \lambda_3} \;\; \frac{\partial H}{\partial \lambda_4} \;\; \frac{\partial H}{\partial \lambda_5} \frac{\partial H}{\partial \lambda_6}\right)^T,$$

with

$$\frac{\partial H}{\partial \lambda_1} = \Lambda + \varepsilon R - \left(\left(1 - u_1(t)\right)\frac{\nu B}{K+B} + \mu\right) S,$$

$$\frac{\partial H}{\partial \lambda_2} = \left(1 - u_1(t)\right)\frac{\rho \nu B}{K+B} S - (\phi + u_2(t) + \theta + \eta_1 + \mu) I_c,$$

$$\frac{\partial H}{\partial \lambda_3} = (1 - u_1)\frac{(1-\rho)\nu B}{K+B} S + (1 - u_2(t))\theta I_c - (\tau + u_3(t) + \beta + \eta_2 + \delta + \mu) I,$$

$$\frac{\partial H}{\partial \lambda_4} = \beta I - (\alpha + u_3(t) + \eta_3 + \mu) C,$$

$$\frac{\partial H}{\partial \lambda_5} = \phi I_c + (\tau + u_3(t)) I + \left(\alpha + u_3(t)\right) C - (\varepsilon + \mu) R,$$

$$\frac{\partial H}{\partial \lambda_6} = \eta_1 I_c + \eta_2 I + \eta_3 C - \mu_b B.$$

Costate equation:

$$\dot{\boldsymbol{\lambda}} = -\frac{\partial H}{\partial \boldsymbol{x}} = \left(-\frac{\partial H}{\partial S} \;\; -\frac{\partial H}{\partial I_c} \;\; -\frac{\partial H}{\partial I} \;\; -\frac{\partial H}{\partial C} \;\; -\frac{\partial H}{\partial R} \;\; -\frac{\partial H}{\partial B}\right)^T,$$

with

$$\dot{\lambda}_1 = \frac{(\lambda_1 - \lambda_3)\nu B + (\lambda_3 - \lambda_2)\rho \nu B + (\lambda_3 - \lambda_1)\nu B u_1(t) + (\lambda_2 - \lambda_3)\rho \nu B u_1(t)}{K+B} + \lambda_1 \mu,$$

$$\dot{\lambda}_2 = (\lambda_2 - \lambda_5)\phi + (\lambda_2 - \lambda_3)\theta + (\lambda_2 - \lambda_6)\eta_1 + \lambda_2 \mu + \lambda_2 u_2 + \lambda_3 u_2 \theta - A_1,$$

$$\dot{\lambda}_3 = (\lambda_3 - \lambda_4)\beta + (\lambda_3 - \lambda_5)\tau + (\lambda_3 - \lambda_6)\eta_2 + \lambda_3(\delta + \mu) + (\lambda_3 - \lambda_5)u_3 - A_2,$$

$$\dot{\lambda}_4 = (\lambda_4 - \lambda_5)\alpha + (\lambda_4 - \lambda_6)\eta_3 + (\lambda_4 - \lambda_5)u_3 + \lambda_4\mu - A_3,$$

$$\dot{\lambda}_5 = (\lambda_5 - \lambda_1)\varepsilon + \lambda_5\mu,$$

$$\dot{\lambda}_6 = \lambda_6\mu_b + \frac{(\lambda_1 - \lambda_3)\nu KS + (\lambda_2 - \lambda_3)\nu\rho\, u_1(t)KS + (\lambda_3 - \lambda_2)\nu\rho\, KS + (\lambda_2 - \lambda_3)\nu\, u_1(t)KS}{(K+B)^2}.$$

In stationary conditions, optimal control $u_i(t)$ must minimize the Hamiltonian form for every time t. This is caused by a condition that should be fulfilled, that is, the first derivative of the Hamiltonian toward each control $u_i(t)$ must be equal to zero, then

$$\frac{\partial H}{\partial \boldsymbol{u}} = \begin{pmatrix} \frac{\partial H}{\partial u_1} & \frac{\partial H}{\partial u_2} & \frac{\partial H}{\partial u_3} \end{pmatrix}^T = (0 \quad 0 \quad 0)^T,$$

with $u_1 = \frac{(\lambda_3 - \lambda_1)\nu BS + (\lambda_2 - \lambda_3)\nu\rho BS}{(K+B)w_1}, u_2 = \frac{(\lambda_3\theta - \lambda_2)I_c}{w_2}, u_3 = \frac{(\lambda_4 - \lambda_5)C + (\lambda_3 - \lambda_5)I}{w_3}$.

Based on the boundary conditions for u_1, u_2, and u_3, which are $0 \le u_1 \le 1,\ 0 \le u_2 \le 1, 0 \le u_3 \le 1$ it is obtained optimal control ${u_1}^*, {u_2}^*$ and ${u_3}^*$ is written as follows:

(1) For control $u_1(t)$:

$${u_1}^*(t) = \begin{cases} 0 & if\ u_1 \le 0 \\ u_1 & if\ 0 < u_1 < 1, \\ 1 & if\ u_1 \ge 1 \end{cases}$$

or

$${u_1}^*(t) = min\left\{1, max\left\{0, \frac{(\lambda_3 - \lambda_1)\nu BS + (\lambda_2 - \lambda_3)\nu\rho BS}{(K+B)w_1}\right\}\right\}.$$

(2) For control $u_2(t)$:

$${u_2}^*(t) = \begin{cases} 0 & if\ u_2 \le 0 \\ u_2 & if\ 0 < u_2 < 1, \\ 1 & if\ u_2 \ge 1 \end{cases}$$

or

$${u_2}^*(t) = min\left\{1, max\left\{0, \frac{(\lambda_2 - \lambda_3)\theta I_c}{w_2}\right\}\right\}.$$

(3) For control $u_3(t)$:

$${u_3}^*(t) = \begin{cases} 0 & if\ u_3 \le 0 \\ u_3 & if\ 0 < u_3 < 1, \\ 1 & if\ u_3 \ge 1 \end{cases}$$

or

$${u_3}^*(t) = min\left\{1, max\left\{0, \frac{(\lambda_4 - \lambda_5)\tau I}{w_3}\right\}\right\}.$$

3.4 Numerical Simulation

The simulation was carried out using the values given in Table 1. We use the forward-backward sweep Runge Kutta Order 4 method and solve for the optimized system numerically. The initial values of each population are $S(0) = 3000$, $I_c(0) = 150$, $I(0) = 350$, $C(0) = 30$, $R(0) = 450$ and $B(0) = 5000$. The individual weights to be minimized $A_1 = A_2 = A_3 = 50$ for reasons of importance in minimizing each infected population are the same. W_1 is the weight of the cost of the health campaign, W_2 is the weight of the cost of screening, and W_3 is the weight of the cost of treatment. It is assumed that the cost weight required for each control to control the spread of typhoid fever is $W_1 = 9$, $W_2 = 7$ dan $W_3 = 10$, where the weight of the cost for complete treatment in reducing the possibility of individuals becoming carrier chronic is more expensive than the weight of the cost health campaign and screening. Changes in the subpopulation before and after being given control are shown in Figure 2-5.

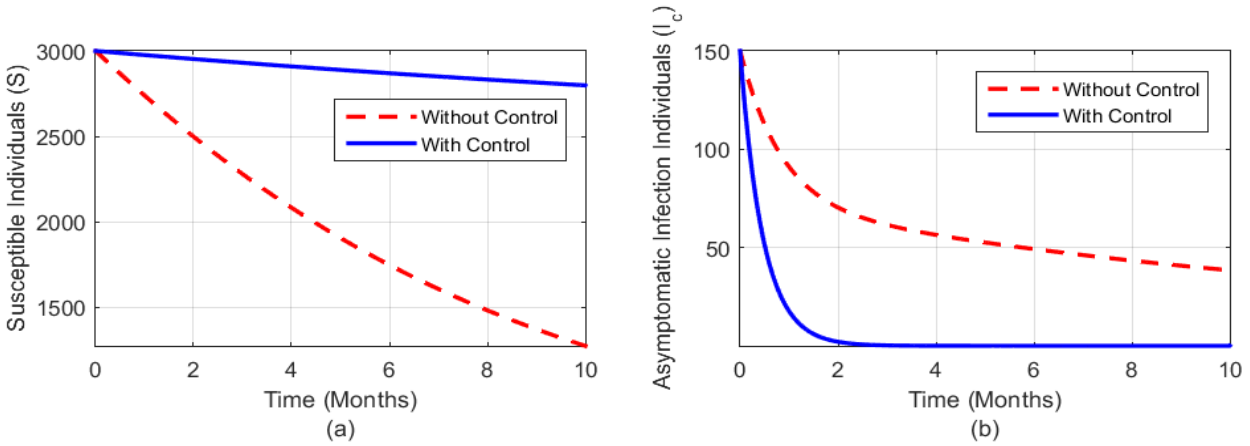

Figure 2. (a) Numerical Simulation of Susceptible Individuals (S), (b) Numerical Simulation of Asymptomatic Infection Individuals (I_c).

Based on Figure 2a graph of susceptible individuals (S) without control decreases rapidly from the beginning to the end of the observation time. Reducing susceptible individuals, (S) was caused by the absence of intervention to suppress the infection rate of the entry individuals S into the subpopulation I and I_c as a result, asymptomatic infection individuals (I_c) and symptomatic infection individuals (I) tend to decrease slowly towards the endemic equilibrium point, (Figure 2b) and (Figure 3a). Reducing the asymptomatic infection individuals (I_C) and symptomatic infection individuals (I) at the beginning of the observation was due to the natural death and recovery rates. Without health campaign control, susceptible individuals (S) that enter the asymptomatic infection individuals (I_c) and symptomatic infection individuals (I) will increase.

The graph with the blue line shows the changes in each subpopulation after being given control health campaigns u_1, screening u_2, and treatment u_3. In Figure 2a, the graph with optimal control shows that the behavior of the susceptible individuals (S) with optimal control tends to decrease slowly from the beginning until the end of observation. This is due to the intervention given to the

rate of infection so that it can reduce the rate of entry of susceptible individuals (S) into asymptomatic infection individuals (I_c) and symptomatic infection individuals (I), which means that health campaign control (u_1) can provide an understanding for the community to apply a clean living culture, personal hygiene and always maintain sanitation. In Figure 2b, the graph with optimal control shows that the behavior of the asymptomatic infection individuals (I_c) tends to decrease in the first five months. In the following month, the asymptomatic infection individuals (I_c) do not change. In addition to the impact of providing health campaigns, the decline in the number of asymptomatic infected individuals (I_c) also is due to the effect of delivering screening control u_2, which is quite effective early so that it allows the asymptomatic infected individuals (I_c) to decrease and enter the symptomatic infection individuals (I) to receive treatment immediately.

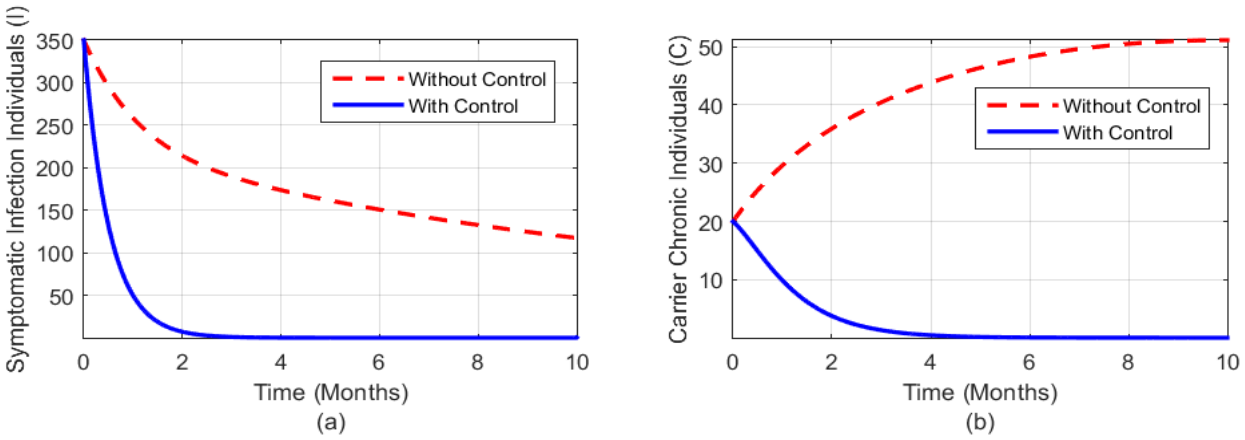

Figure 3. (a) Numerical Simulation of Symptomatic Infection Individuals $(\boldsymbol{I})$, (b) Numerical Simulation of Chronic Carrier Individuals $(\boldsymbol{C})$.

Based on Figure 3a, the graph with optimal control shows that the symptomatic infection individuals (I) began to decrease rapidly in the first months and did not change in the next month. The decrease in symptomatic infection individuals(I) is not only caused by control in the form of health campaigns but also due to control in the form of treatment u_3 that can increase recovered individuals (R) and reduce the proportion of symptomatic infection individuals (I) entering to carrier individuals (C). Figure 3b shows that the graph behavior of carrier individuals (C) without control increases in the following month until the end of the observation. Increasing the carrier individuals (C) is due to the absence of intervention given to the rate of treatment. In Figure 3b, the graph of the subpopulation C with control tends to decrease from the beginning until the end of observation. This shows that the provision of control in the form of treatment (u_3) can reduce the entry of symptomatic individuals (I) to carrier individuals (C).

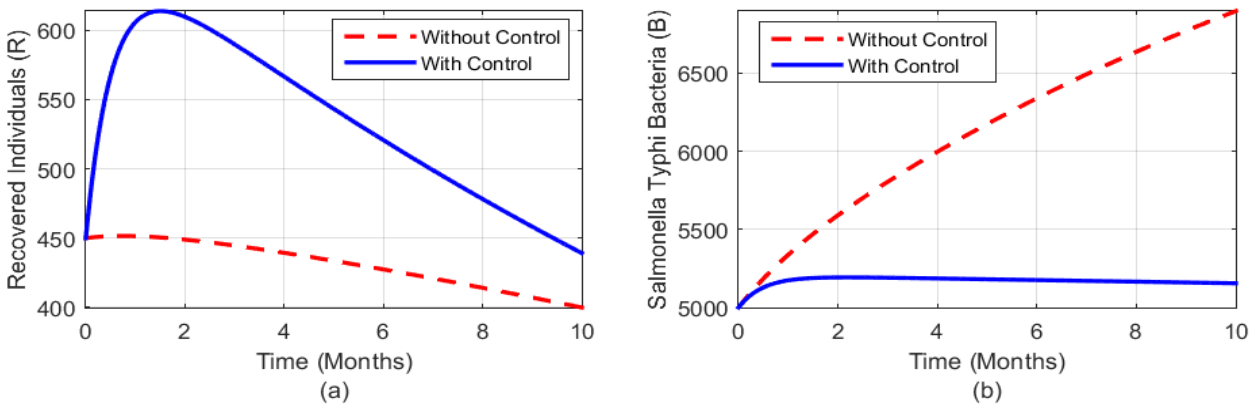

Figure 4. (a) Numerical Simulation of Recovered Individuals $(\boldsymbol{R})$, (b) Numerical Simulation of Salmonella Typhi Bacteria $(\boldsymbol{B})$.

In Figure 4a, recovered individuals (R) without control tend to decrease rapidly from the observation time until the end of the observation. In contrast, the graph with control tends to increase in the first two months of observation and then decline again in the following month. The increase of recovered individuals (R) with control was caused by the presence of individuals recovering after performing and natural recovery rate in the asymptomatic infection individuals (I_c) and carrier individuals (C). In Figure 4b, the number of Samonellah Thypii bacteria in the environment (B) tends to increase from the beginning to the end of the observation. The increase in the number of bacteria is in line with the rise in asymptomatic infection individuals (I_c), symptomatic infection individuals (I), and carrier individuals (C). This is because no health campaign u_1 is provided to the community, impacting infected individuals and the disposal of environmental bacteria. In Figure 2f, the graph with control, the Salmonella Thypi bacteria (B) population increase only in the first two months. In the following month, the bacterial population in the environment did not change. Health campaigns can provide understanding for the community to apply a culture of clean living, personal hygiene, and always maintaining sanitation.

Based on Figure 5, health campaign control (u_1) should be given maximally from the observation's beginning to the end. Screening control (u_2) should be given maximally for three months, and in the following month, the screening can be reduced slowly. The graph of the treatment control function(u_3) should be given maximally in the first five months of observation. After that, the following month of treatment (u_3) can be decreased to the end of the observation.

Furthermore, it will discuss the accumulation of infected individuals from each infected subpopulation before and after being given control of the health campaign, screening, and treatment for ten months. The number of infected individuals from each subpopulation was calculated using the Riemann integral by partitioning the estimated area into 10000 parts with a rectangular shape which will be presented in Table 3. Based on Table 3, applying control for ten months can reduce as many as 98.14% of individuals I_c without control, 89.82% of individuals I without control, and 94.21% of individuals C without control.

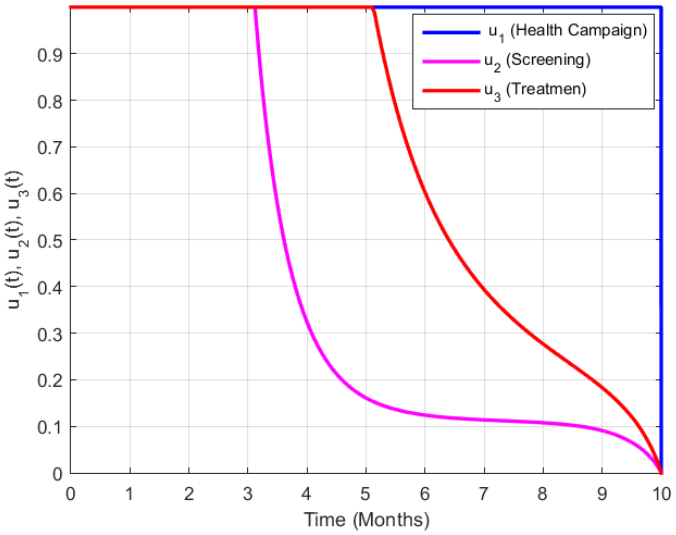

Figure 5. The Function of Health Campaigns Control $(\boldsymbol{u_1})$, screening $(\boldsymbol{u_2})$ and treatment $(\boldsymbol{u_3})$.

Table 3. Accumulation of Infected Individuals

Treatment	Subpopulation		
	I_c	I	C
Without Control	598	1769	432
With Control u_1, u_2 dan u_3	70	180	25

4. CONCLUSIONS

The developed mathematical model yields non-endemic and endemic equilibrium points. Endemic and non-endemic equilibrium points are asymptotically stable if they meet the conditions set by the Routh-Hurwitz rule. The simulation results with the application of controls in the form of a health campaign, screening, and treatment indicate that the number of asymptomatic individuals can be reduced by as much as 98.14%, symptomatic individuals by as much as 89.82%, and chronic carrier individuals as much as 94.21%. The use of screening and treatment controls is less important when compared to health campaign controls. The use of controls in the form of health campaigns has a more significant influence when compared to controls in the form of screening and treatment. This shows that prevention in the form of health campaigns must be carried out for a long time to prevent the spread of typhoid fever. Meanwhile, the control of treatment effectively reduces the number of symptomatic individuals from becoming chronic carriers. Based on the results of numerical simulations, the most effective strategy in controlling the spread of typhoid fever is to simultaneously apply controls in the form of health campaigns, screening, and treatment.

REFERENCES

[1] OMS, "Données épidémiologiques sur la typhoïde," pp. 153–172, 2018.

[2] WHO, "Typhoid and other invasive salmonellosis," 2018. [Online]. Available: https://www.who.int/publications/m/item/vaccine-preventable-diseases-surveillance-standards-typhoid. [Accessed 03 May 2022].

[3] K. A. A. Prayoga and N. N. D. Fatmawati, "Identifikasi Salmonella spp pada feses penjamah makanan di rumah potong ayam RJ dengan metode kultur," *Intisari Sains Medis,* vol. 9, no. 3, pp. 1-5, 2018.

[4] W. Mulu et al., "Seroconfirmed Typhoid Fever and Knowledge, Attitude, and Practices among Febrile Patients Attending at Injibara General Hospital, Northwest Ethiopia," *BioMed Res. Int.,* vol. 2, no. Article ID 8887266, pp. 1-8, 2021. https://doi.org/10.1155/2021/8887266.

[5] J. S. Gauld, H. Hu, D. J. Klein and M. M. Levine, "Typhoid fever in Santiago, Chile: Insights from a mathematical model utilizing venerable archived data from a successful disease control program," *PLoS Negl. Trop. Dis.,* vol. 12, no. 9. p. e0006759, 2018. doi: 10.1371/journal.pntd.0006759.

[6] S. T. Tresna, Subiyanto and S. Supian, "Mathematical Models for Typhoid Disease Transmission: A Systematic Literature Review," *Mathematics,* vol. 10, no. 14, p. 2506, 2022, doi: 10.3390/math10142506.

[7] J. S. Gunn, J. M. Marshall, S. Baker, S. Dongol, R. C. Charles and E. T. Ryan, "Salmonella chronic carriage: epidemiology, diagnosis, and gallbladder persistence," *Trends Microbiol,* vol. 22, no. 11, p. 648–655, 2014.

[8] V. Gupta, M. Kaur, P. Datta and J. Chander, "Chronic urinary carrier state due to Salmonella Typhi causing urinary tract infection in an immunocompetent healthy woman," *Trop. Doct.,* vol. 48, no. 3, p. 236–238, 2018.

[9] S. C. Olsen, P. Boggiatto, J. Wilson-Welder, P. Nol, J. Rhyan and N. Srirangathan, "Immunogenicity and Efficacy of a Rough Brucella suis Vaccine Delivered Orally or Parenterally to Feral Swine," *International Journal of Vaccine Research,* vol. 2, no. 1, p. 6, 2017.

[10] C. H. Watson and W. J. Edmunds, "A review of typhoid fever transmission dynamic models and economic evaluations of vaccination," *Vaccine,* vol. 33, p. C42–C54, 2015, doi: 10.1016/j.vaccine.2015.04.013.

[11] S. Toaha, Pemodelan Matematika dalam Dinamika Populasi, Makassar: Dua Satu Pers, 2013.

[12] K. Kasbawati, "Kontrol Optimal Upaya Pencegahan Infeksi Virus Flu Burung H5N1 dalam Populasi Burung dan Manusia," *J. Mat. Stat. Dan Komputasi,* vol. 8, no. 1, pp. 12-24, 2011.

[13] O. J. Peter, A. F. Adebisi, M. O. Ajisope, F. O. Ajibade, A. I. Abioye and F. A. Oguntolu, "Global Stability Analysis of Typhoid Fever Model," *Adv. Syst. Sci. Appl.,* vol. 20, no. 2, p. Art. no 2, 2020, doi: 10.25728/assa.2020.20.2.792.

[14] H. O. Nyaberi and J. S. Musaili, "Mathematical modeling of the impact of treatment on the dynamics of typhoid," *J. Egypt. Math. Soc.,* vol. 29, no. 1, pp. 1-11, 2021.

[15] G. T. Tilahun, O. D. Makinde and D. Malonza, "Modelling and optimal control of typhoid fever disease with cost-effective strategies," *Computational and Mathematical Methods in Medicine,* vol. 1, pp. 1-16, 2017.

[16] J. Mushanyu, F. Nyabadza, G. Muchatibaya, P. Mafuta and G. Nhawu, "Assessing the potential impact of limited public health resources on the spread and control of typhoid," *J. Math. Biol.,* vol. 77, no. 3, p. 647–670, 2018.

[17] S. Mushayabasa, C. P. Bhunu and E. T. Ngarakana-Gwasira, "Assessing the impact of drug resistance on the transmission dynamics of Typhoid fever," *Comput. Biol. J.,* vol. 2013, 2013.

[18] C. B. Acosta-Alonzo, I. V. Erovenko, A. Lancaster, H. Oh, J. Rychtář and D. Taylor, "High endemic levels of typhoid fever in rural areas of Ghana may stem from optimal voluntary vaccination behaviour," *Proc. R. Soc. A,* vol. 476, no. 2241, p. p. 20200354, 2020.

[19] A. S. Shaikh and K. S. Nisar, "Transmission dynamics of fractional order Typhoid fever model using Caputo–Fabrizio operator," *Chaos Solitons Fractals,* vol. 128, p. 355–365, Nov. 2019, doi: 10.1016/j.chaos.2019.08.012.

[20] H. Abboubakar and R. Racke, "Mathematical modeling, forecasting, and optimal control of typhoid fever transmission dynamics," *Chaos Solitons Fractals,* vol. 149, p. 111074, 2021.

[21] T. A. Ayoola, H. O. Edogbanya, O. J. Peter, F. A. Oguntolu, K. Oshinubi and M. L. Olaosebikan, "Modelling and optimal control analysis of typhoid fever," *J. Math. Comput. Sci.,* vol. 11, no. 6, pp. 6666-6682, 2021.

[22] J. T. Workman and S. Lenhart, Optimal Control Applied to Biological Models, in Optimal Control Applied to Biological Models, London: Taylor & Francis Group, 2007.